

Inhibitor Complexes of the *Pseudomonas* Serine-Carboxyl Proteinase[†]

Alexander Wlodawer,^{*,‡} Mi Li,^{‡,§} Alla Gustchina,[‡] Zbigniew Dauter,^{||} Kenichi Uchida,[⊥] Hiroshi Oyama,[#]
Nathan E. Goldfarb,[∇] Ben M. Dunn,[∇] and Kohei Oda[#]

Protein Structure Section, Macromolecular Crystallography Laboratory, and Intramural Research Support Program, SAIC Frederick, National Cancer Institute at Frederick, Frederick, Maryland 21702, Synchrotron Radiation Research Section, Macromolecular Crystallography Laboratory, National Cancer Institute and NSLS, Brookhaven National Laboratory, Building 725A-X9, Upton, New York 11973, Department of Biosciences, School of Science and Engineering, Teikyo University, 1-1 Toyosatodai, Utsunomiya, 320-8551, Japan, Department of Applied Biology, Faculty of Textile Science, Kyoto Institute of Technology, Sakyo-ku, Kyoto 606-8585, Japan, and Department of Biochemistry and Molecular Biology, University of Florida, Gainesville, Florida 32610

Received September 19, 2001

ABSTRACT: Crystal structures of the serine-carboxyl proteinase from *Pseudomonas* sp. 101 (PSCP), complexed with a number of inhibitors, have been solved and refined at high- to atomic-level resolution. All of these inhibitors (tyrostatin, pseudo-tyrostatin, AcIPF, AcIAF, and chymostatin, as well as previously studied iodotyrostatin and pseudo-iodotyrostatin) make covalent bonds to the active site Ser287 through their aldehyde moieties, while their side chains occupy subsites S1–S4 of the enzyme. The mode of binding of the inhibitors is almost identical for their P1 and P2 side chains, while significant differences are observed for P3 and P4 (if present). Kinetic parameters for the binding of these nanomolar inhibitors to PSCP have been established and correlated with the observed mode of binding. The preferences of this enzyme for a larger side chain in P2 as well as Tyr or Phe in P1 are explained by the size, shape, and characteristics of the S2 and S1 regions of the protein structure, respectively. Networks of hydrogen bonds involving glutamic and aspartic acids have been analyzed for the atomic-resolution structure of the native enzyme. PSCP contains a calcium-binding site that consists of Asp328, Asp348, three amide carbonyl groups, and a water molecule, in almost perfect octahedral coordination. The presence of Ca²⁺ cation is necessary for the activity of the enzyme.

Serine-carboxyl proteinases belong to a recently characterized family of proteolytic enzymes that share their fold with subtilisin, but contain an active site with a unique catalytic triad, Ser-Glu-Asp (1, 2). This family was previously known as pepstatin-insensitive carboxyl proteinases (3–6), in view of the importance of a number of aspartic and glutamic acid residues for their catalytic activity; the current name was introduced after the structure of its first member was determined. Other related bacterial enzymes include *Xanthomonas* sp. T-22 carboxyl proteinase (XSCP) (3), kumamolysin (KSCP), an enzyme isolated from a thermophilic bacterium *Bacillus novosp.* MN-32 (7), and alcohol-resistant proteinase J-4, isolated from *Bacillus coagulans* (8). An important member of this class of proteinases is CLN2, a

mammalian tripeptidyl-peptidase I (9, 10), which, when mutated, leads to a fatal human neurodegenerative disease, classical late-infantile neuronal ceroid lipofuscinosis (11). Lys60 and Lys45, markers for late lysosomes in *Amoeba proteus* (12), are also putative members of this family.

Our previous studies have resulted in the structure of the uninhibited enzyme solved and refined at 1 Å resolution, as well as in the 1.4 Å structure of a covalent complex of PSCP with an inhibitor. Surprisingly, although the inhibitor that was used for preparation of the crystals was nominally iodotyrostatin (Figure 1A), we found that the electron density corresponded to a shorter peptide, named pseudo-iodotyrostatin (Figure 1B). Since characterization of the inhibitor sample by mass spectrometry and NMR has shown that the former compound predominated in the sample that was used for cocrystallization (purity at least 95%), we concluded that the binding of pseudo-iodotyrostatin, a putative contaminant of the sample, must have been much stronger. This conclusion, however, needed further structural and enzymatic verification. In addition, several new compounds were synthesized for the purpose of inhibiting KSCP, an enzyme whose structure is under crystallographic investigation (W. Bode, personal communication). We were interested to see if these new compounds, AcIPF¹ (Figure 1C) and AcIAF (Figure 1D), would also inhibit PSCP and to what extent. We also decided to investigate the equilibrium parameters of the noniodinated versions of tyrostatin and pseudo-

[†] This work was supported in part by Grant-in-Aid for Scientific Research (B) 13460043 from the Ministry of Education, Science, Sports and Culture of Japan (to K.O.), by NIH Grants DK18865 and AI28571 (to B.M.D.), and with federal funds from the National Cancer Institute, National Institutes of Health, under Contract NO1-CO-56000.

* Correspondence should be addressed to this author. E-mail: wlodawer@ncifcrf.gov.

[‡] Protein Structure Section, National Cancer Institute at Frederick.

[§] Intramural Research Support Program, National Cancer Institute at Frederick.

^{||} National Cancer Institute and NSLS, Brookhaven National Laboratory.

[⊥] Department of Biosciences, Teikyo University.

[#] Department of Applied Biology, Kyoto Institute of Technology.

[∇] Department of Biochemistry and Molecular Biology, University of Florida.

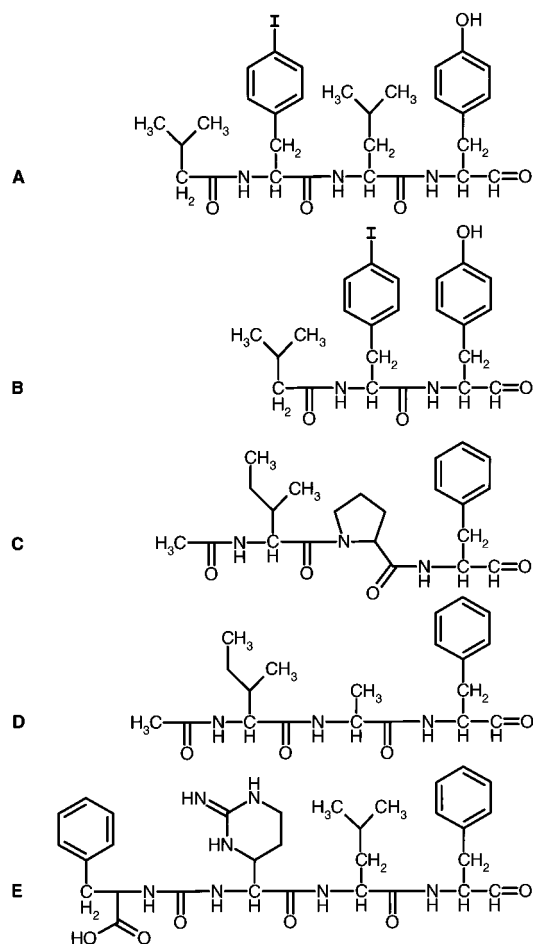


FIGURE 1: Chemical formulas of the inhibitors used in this study. (A) Iodotyrostatin (in tyrostatin, I is replaced by OH); (B) pseudoiodotyrostatin (in pseudo-tyrostatin, I is replaced by OH); (C) AcIPF; (D) AcIAF; and (E) chymostatin.

tyrostatin, as well as chymostatin (Figure 1E), an inhibitor of serine proteinases that has been previously studied in complexes with several enzymes (13, 14). These kinetic and structural data are presented and discussed below.

MATERIALS AND METHODS

Synthesis of Inhibitors. The peptides used as intermediates in the synthesis of inhibitors were synthesized by the liquid-phase DCC–HOBt method. The structures of the products were confirmed mainly by ^1H NMR spectroscopy using the EX-400 (JEOL) instrument.

(A) *Isoval-Tyr(tBu)-Leu-Tyr(tBu)-OMe*. The peptide Z-Tyr(tBu)-Leu-Tyr(tBu)-OMe (6.0 g, 836 mmol, in 100 mL of methanol) was hydrogenated under atmospheric pressure with 10% Pd/C (0.6 g) for 4 h at room temperature. Subsequently 10% Pd/C (0.6 g) was added to 6.0 g (8.36 mmol) in 100 mL of methanol and hydrogenated under atmospheric pressure for 4 h at room temperature. After removing the catalyst by filtration, the solvent was evaporated in vacuo. The residual syrup was dissolved in dichloromethane (30 mL), and isovaleryl anhydride (2.3 g, 12.3

mmol) in dichloromethane (20 mL) was added to this solution followed by triethylamine (3.5 mL) in an ice/water bath, and stirred overnight at room temperature. The white precipitate was filtered and washed with cold methanol and dried over P_2O_5 in vacuo, with the final yield of 5.0 g (86%), melting point (mp) 241.4–242.8 °C.

(B) *Isoval-Tyr(tBu)-Leu-(O^t-tert-butyl)tyrosinol*. LiCl (0.61 g, 16 mmol) and NaBH_4 (0.68 g, 16 mmol) were added to the solution of isoval-Tyr(tBu)-Leu-Tyr(tBu)-OMe (2.5 g, 3.74 mmol) in a mixture of ethanol (32 mL) and tetrahydrofuran (16 mL) and stirred for 3 h at room temperature. The solution was carefully acidified with 1 N HCl to pH 2, and the solvent was evaporated to half its volume. The solution was extracted with ethyl acetate, and the organic phase was washed with water, and then dried on anhydrous sodium sulfate. After evaporation, the product was crystallized by adding hexane and recrystallized from dichloromethane/hexane, with yield of 2.2 g (96%), mp 226.9–228.3 °C.

(C) *Isoval-Tyr-Leu-tyrosinol*. Isoval-Tyr(tBu)-Leu-(O^t-tert-butyl)tyrosinol (513 mg, 1 mmol) was dissolved in 90% trifluoroacetic acid (5 mL). After 1.5 h, the solvent was evaporated. The residual syrup was purified by a silica gel column (Silica Gel 60, Merck, 3 × 20 cm) eluted with chloroform/methanol 15:1, with the final yield of 313 mg (61%), mp 215.0–215.9 °C.

(D) *Isoval-Tyr-Leu-Tyr-H (Tyrostatin)*. To the solution of isoval-Tyr-Leu-tyrosinol (200 mg, 0.39 mmol) in DMSO (1 mL) with triethylamine (157 mg, 1.56 mmol) was added sulfur trioxide pyridine complex (248 mg, 1.56 mmol) in DMSO (1 mL) (15, 16). After stirring for 15 min at room temperature, the reaction mixture was poured into ice/water and extracted with ethyl acetate. The organic layer was successively washed with 10% aqueous citric acid, water, saturated aqueous sodium hydrogen carbonate, and water. After drying on anhydrous sodium sulfate, the solvent was evaporated, and the product was crystallized with hexane and recrystallized from dichloromethane/hexane. Yield 137 mg (69%); mp 146.3–147.5 °C.

(E) *Isoval-Tyr-Tyr-H (pseudo-tyrostatin)* was made by the same method as tyrostatin, with the final yield of 123 mg (62%); mp 83.5–84.7 °C.

(F) *Ac-Ile-Ala-Phe-H (AcIAF)* was obtained in an analogous way by oxidation of Ac-Ile-Ala-phenylalaninol (338 mg, 1 mmol) with a yield of 145 mg (38%); mp 187.8 °C (decomposition).

(G) *Ac-Ile-Pro-Phe-H (AcIPF)* was obtained from Ac-Ile-Pro-phenylalaninol (404 mg, 1 mmol) oxidized in an analogous manner. The dichloromethane solution of the product was evaporated and dried on P_2O_5 in vacuo, yielding amorphous material (300 mg, 74%).

(H) *Boc-tyrosinol*. Boc-Tyr-OMe (5.9 g, 20 mmol) was reduced with LiCl (3.4 g, 80 mmol) and NaBH_4 (3.0 g, 80 mmol) overnight at room temperature in ethanol/tetrahydrofuran (150 mL/100 mL). After evaporating a half volume of solvent, the solution was carefully acidified with 10% citric acid to pH 3. The solution was extracted with ethyl acetate, and the organic phase was washed with 10% citric acid and water, and then dried on anhydrous sodium sulfate and recrystallized from ethyl acetate/hexane, yielding 4.9 g (91%), mp 97.0–98.6 °C.

¹ Abbreviations: Ac, acetyl; Boc, *tert*-butoxycarbonyl; DCC, *N,N'*-dicyclohexylcarbodiimide; DMSO, dimethyl sulfoxide; DOX, 1,4-dioxane; HOBt, 1-hydroxybenzotriazole; isoval, isovaleryl; isoval-OSu, *O*-isovalerylhydroxysuccinimide; Phe(4-I), 4-iodophenylalanine; tBu, *tert*-butyl; Z, benzylloxycarbonyl.

(I) *Boc-(O¹,O⁴-diacetyl)tyrosinol*. Acetic anhydride (10 mL) was added dropwise for 20 min at room temperature to the solution of Boc-tyrosinol (4.54 g, 17 mmol) in pyridine (20 mL). After 5 h, the reaction mixture was poured into ice/water and extracted with ethyl acetate. The organic layer was successively washed with 1 N HCl, water, saturated aqueous sodium hydrogen carbonate, water, and brine, and then dried on anhydrous sodium sulfate and crystallized from ethyl acetate/hexane (yield 5.4 g, 90%), mp 114.5–114.9 °C.

(J) *Boc-Phe(4-I)-(O¹,O⁴-diacetyl)tyrosinol*. Boc-Phe(4-I)-OH (3.91 g, 10 mmol) and *O¹,O⁴-diacetyl*tyrosinol, which was prepared from Boc-(*O¹,O⁴-diacetyl*)tyrosinol (3.51 g, 10 mmol), were coupled by the DCC–HOBt method, with a yield of 2.6 g (42%), mp 169.0–171.2 °C.

(K) *Isoval-Phe(4-I)-(O¹,O⁴-diacetyl)tyrosinol*. Boc-Phe(4-I)-(O¹,O⁴-diacetyl)tyrosinol (2.49 g, 4 mmol) was treated with 4 N HCl/DOX (15 mL) for 2 h at room temperature. The solvent was evaporated and dried over NaOH in vacuo. The residue was dissolved in dimethoxyethane (8 mL), triethylamine (0.41 g, 4 mmol), and isoval-OSu (0.79 g, 4.1 mmol) was added on an ice/water bath. After stirring overnight, the reaction mixture was poured into ice/water. The precipitate was filtered and recrystallized from methanol, yielding 1.0 g (40%), mp 212.7–214.0 °C.

(L) *Isoval-Phe(4-I)-tyrosinol*. NaOH (1 N, 3 mL) was added dropwise at 0 °C to the suspension of isoval-Phe(4-I)-(O¹,O⁴-diacetyl)tyrosinol (0.91 g, 1.5 mmol) in methanol (12 mL). The solution was stirred for 2 h, and then the solvent was evaporated to half a volume. The mixture was poured into ice–water and stored overnight at 4 °C. The precipitate was filtered and washed with water, yielding 0.77 g (98%), mp 213.4–214.1 °C.

(M) *Isoval-Phe(4-I)-Leu-tyrosinol*. Isoval-Phe(4-I)-Leu-(O¹,O⁴-diacetyl) tyrosinol (1.08 g, 1.5 mmol) was hydrolyzed by the same method as isoval-Phe(4-I)-tyrosinol, yielding 0.94 g (98%), mp 232.4–232.9 °C.

(N) *Isoval-Phe(4-I)-Leu-Tyr-H (iodotyrostatin)* was prepared by oxidation of isoval-Phe(4-I)-Leu-tyrosinol (100 mg, 0.157 mmol) by the same method as utilized to prepare tyrostatin. The yield was 47 mg (47%); mp 226.0 °C (decomposition).

(O) *Isoval-Phe(4-I)-Tyr-H (pseudo-iodotyrostatin)* was obtained by oxidation of isoval-Phe(4-I)-tyrosinol (0.20 g, 0.41 mmol). The yield was 80 mg (40%); mp 155.7–157.1 °C.

Protein Purification, Complex Formation, and Crystallization of PSCP. Protein used in these studies was over-expressed in *Escherichia coli* and purified as described elsewhere (4). We have initially obtained three crystal forms of PSCP under different conditions (I); only crystals identified as Form III were used in this study. All crystals were grown using a complex of PSCP with an inhibitor sample that nominally contained iodotyrostatin (Figure 1A). The complex was prepared by mixing 17.7 mg of PSCP dissolved in 950 mL of 50 mM sodium acetate buffer, pH 4.8, also containing 5 mM CaCl₂ and 0.1 M NaCl, with inhibitor solution (31 mg dissolved in 50 mL of DMSO solution). After 2 h incubation, the residual activity was 15%. At that stage, 2 mg of inhibitor in 0.6 mL of DMSO was again added, but the residual activity was not further diminished after 30 min. The reaction mixture was concentrated with

an Amicon Centriflo CF25 using a Hitachi refrigerated centrifuge model CR21E (1000g at 4 °C for 1 day) to the interim concentration of 0.84 mg/mL (total 12.6 mg of the complex) and was stored at 4 °C.

Crystals were grown at room temperature as described before (I, 2). After final concentration, stock solution of the enzyme consisted of 9 mg/mL PSCP dissolved in sodium acetate buffer at pH 4.8, with added 0.1 M NaCl and 5 mM CaCl₂. For each crystallization experiment, stock solution was mixed 1:1 with well solution containing 5% guanidine hydrochloride, 10% glycerol, 5% methanol, and 44–50% ammonium sulfate, 0.1 M sodium acetate buffer, pH 4.3. Guanidine was not used in the growth of crystals that were later soaked with AcIAF and AcIPF.

Exchange of Inhibitors in the PSCP Crystals. The crystals were transferred from their original mother liquor to a new one containing 1.6 M Li₂SO₄ at pH 7.5 and were kept in that solution for approximately 30 min. This procedure was based on our previous observation indicating that the covalently bound inhibitor (hemiacetal) reversibly dissociates at such pH, as monitored by the disappearance of any density that could be attributed to the inhibitor in the electron density maps (data not shown). The crystals were subsequently transferred to another mother liquor containing 1.2 M ammonium sulfate, 10% glycerol, 5% guanidine hydrochloride, and 5% methanol, at pH 3.32. Stock solutions of inhibitors, prepared by dissolving each inhibitor sample in DMSO at a concentration of 10 mg/mL, were added in turn to the mother liquor at the ratio of 1:10 (volume of inhibitor solution to that of the mother liquid drop). Crystals were soaked in the resulting solution for between 1 h and overnight, and then were used for data collection.

X-ray Data Collection. A majority of the X-ray diffraction data for crystals discussed here were collected on beam line X9B, NSLS, Brookhaven National Laboratory, using the ADSC Quantum4 CCD detector, while some data were collected with a Mar345 detector mounted on a Rigaku Ru200 rotating anode generator, operating at 50 kV and 100 mA. The reflections were integrated and merged using the HKL2000 suite (17), with the results summarized in Table 1.

Refinement of the Models. The atomic models of the inhibitor complexes of PSCP presented here, as well as the structures described previously (2), were all refined according to similar protocols using the program SHELXL (18). The refinement was performed against F-squared in the conjugate gradient (CGLS) mode. After each round of refinement, the models were compared with the respective electron density maps and modified using the interactive graphics display programs QUANTA (Molecular Simulations Inc., San Diego) or O (19). The default SHELXL restraints were used for geometrical (20) and displacement parameters. At first, the models were refined isotropically to convergence and then anisotropically, with the exception of the structures refined at the resolution lower than 1.5 Å. The introduction of anisotropic displacement parameters in high-resolution refinement was validated by the drop in both R_{cryst} and R_{free} . Hydrogen atoms were introduced as rigidly “riding” on their parent atoms, except for side chains in double conformations. Water oxygen atoms were refined with unit occupancies, although some of the sites are probably only partially occupied. The refinement parameters are presented in Table 1.

Table 1: Details of X-ray Data Collection and Refinement

crystal ligand	E tyrostatin	F AcIPF	G AcIAF	H chymostatin	I pseudo-tyrostatin
unit cell dimensions (Å)					
of space group $P6_2$					
$a = b$	97.3	97.25	97.29	97.40	98.27
c	83.0	83.45	83.46	83.35	83.30
wavelength (Å)	0.92	0.92	0.92	1.5418	1.5418
resolution (Å)	1.4	1.1	1.1	2.0	1.8
measured reflections	502477	1117051	1059020	104718	205652
unique reflections	87746	181161	181240	28260	41501
R_{merge} (%)	5.8 (39.9) ^a	5.4 (47.4)	5.9 (51.9)	7.3 (39.6)	4.6 (28.2)
$I/\sigma(I)$	28.6 (3.5)	27.7 (2.9)	28.0 (2.5)	15.7 (2.6)	39.4 (5.8)
completeness (%)	97.4 (99.9)	100.0 (100.0)	100.0 (100.0)	92.4 (93.0)	98.0 (99.1)
	Refinement				
R , no σ cutoff (%)	18.5	13.41	12.97	18.70	15.47
R_{free} (%)	22.6	15.53	14.08	24.26	21.54
rms bond lengths (Å)	0.010	0.018	0.017	0.005	0.009
rms angle distances (Å)	0.027	0.044	0.045	0.022	0.026
protein atom sites	2670	2684	2689	2672	2674
inhibitor atoms	38	29	27	29	29
other ligand atoms ^b	1	19	19	1	1
water sites	419	427	502	206	493
disordered side chains	4	4	4	3	4
s.u. of main chain atoms (Å) ^c	—	0.032	0.037	—	—
PDB accession code	1KDZ	1KDY	1KDV	1KE2	1KE1

^a In parentheses are values in the highest resolution shell. ^b One Ca^{2+} ion is present in all models; three glycerol molecules are also found in models F and G. ^c Average standard uncertainty of atomic positions in the main chain from the inversion of least-squares matrix (only applicable to atomic-resolution structures).

At the end of refinement of the atomic-resolution structures, a round of blocked full-matrix least-squares refinement was performed using all reflections, including those previously used for R_{free} , to obtain as accurate models as possible and to properly estimate the standard uncertainties of all individual refined parameters from the inversion of the least-squares matrixes. The coordinates have been deposited in the Protein DataBank (see Table 1 for accession codes).

Peptide Substrates and Recombinant Enzyme. For enzyme kinetic analyses, stock peptide solutions were made in filtered distilled water and quantified by amino acid analysis (University of Florida Protein Core Facility). The purity of the peptides ($\geq 90\%$) was verified by high-pressure liquid chromatography and MALDI-TOF analysis. For these measurements, recombinant PSCP was diluted in 50 mM sodium acetate, pH 4.8, 5 mM CaCl_2 .

Kinetic Assays Using Competitive Inhibitors. Inhibition constants, K_i , were determined by monitoring the competitive inhibition of the hydrolysis of the peptide Lys-Pro-Ile-Lys-Phe* Nph-Arg-Leu (University of Florida Protein Core Facility) for PSCP. All reactions were performed at 37 °C and a final concentration of 0.1 M sodium formate, pH 3.5, and $\leq 2\%$ DMSO. Initial rates of substrate cleavage with at least six different substrate concentrations were measured following a 10 min preincubation without inhibitor. Next, initial rates were obtained after preincubation with at least two different concentrations of inhibitor and using six different substrate concentrations. Several experiments were done to vary the preincubation time. No differences in the level of inhibition were seen between 10 and 30 min of preincubation. Therefore, we used 10 min in all experiments reported here. The K_i value was calculated from simultaneous fits of all three curves of velocity versus substrate concentration to the equation: $v = V_{\text{max}}[S]/\{K_m(1 + [I]/K_i) + S\}$.

RESULTS AND DISCUSSION

A Calcium-Binding Site of PSCP. A prominent Ca-binding site has been observed in the previously published (2) and the current structures of PSCP, but the mode of binding and the role of this ion have not yet been discussed in any detail. The identity of this ligand is of little doubt, since not only is the metal ion surrounded by an octahedron of atoms in virtually identical positions in all structures discussed here, but also its location corresponds to the most prominent peak in the map based on Bijvoet differences for a data set collected at the wavelength of 1.54 Å (Figure 2) (1). Common Ca-binding sites are either perfectly octahedral or pseudo-octahedral, in which one of the apexes contains two oxygens of a carboxylic group. In PSCP, each apex of the octahedron consists of a single carboxylate oxygen of Asp328 and Asp348. The base of the octahedron consists of three amide carbonyl groups of residues 329, 344, and 346, and a very clearly delineated water molecule (Wat401). All distances between the oxygens and the Ca^{2+} ion refine extremely close to each other (2.28–2.32 Å without any restraints); only the distance to Wat401 is marginally longer (2.40 Å).

Ca-binding sites have been previously reported in every structure of members of the subtilisin family. However, the location of the Ca-binding site is completely different than either the tight or the looser Ca-binding sites in subtilisin Carlsberg, Novo, or its other variants (21–24). The structural role of this site in PSCP may be to tie the long loop containing residues 328–342 to the short loop 343–348, and both of them to the opposite strand around residue 353. The largest part of this region represents a unique insert in PSCP and has no correspondence in subtilisins. Only the base of the loop is involved in binding the Ca^{2+} ion, so that the presence of this site is compatible with loops of different

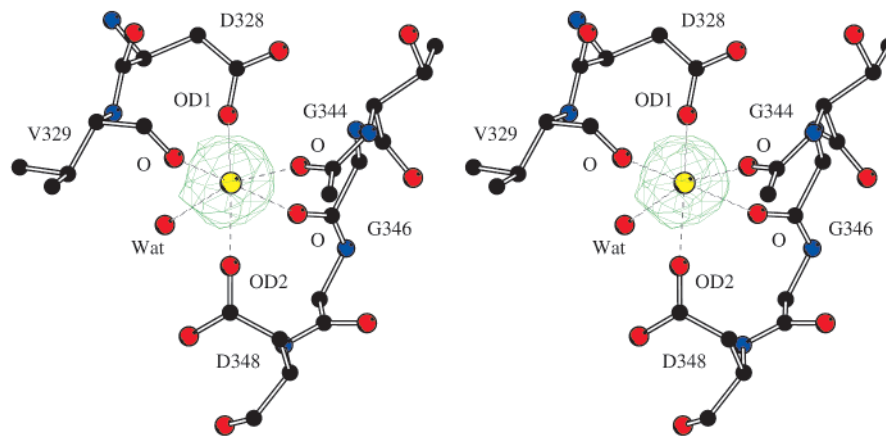


FIGURE 2: Ca-binding site in PSCP. The anomalous electron density map computed using data collected at a wavelength of 1.54 Å and contoured at 5.0 σ level defines unambiguously the position of the ion, and the surrounding residues are shown together with their distances. The distances between Ca²⁺ and the ligands are very similar in all structures discussed here.

length likely present in other members of the PSCP family. The importance of the integrity of the Ca-binding site was verified in the experiments that showed that modifications or mutation of Asp328 abolishes catalytic activity of PSCP, as judged both by the absence of autoprocessing and by the inactivity of the enzyme (6). While the originally proposed catalytic role of Asp328 was not supported by the subsequent structural data, the experiment described above established beyond any doubt the importance of the integrity of the Ca-binding site for the activity of the enzymes. It must be stressed, however, that this site is quite removed from the active site, and the exact mode of interaction of these two regions of the protein is not obvious.

Structural Studies of the Inhibitor Complexes of PSCP. The protein used for crystallization was complexed with an inhibitor, as described under Materials and Methods. However, an analysis of the electron density map resulted in the interpretation that the inhibitor actually bound in the original crystals was not iodotyrostatin (Figure 1A) (25), but rather pseudo-iodotyrostatin (Figure 1B). In the originally reported structure of PSCP (2), crystals were grown at pH 3.5 without excess inhibitor in solution, with the pH not allowed to increase at any stage of the procedure; nevertheless, the resulting occupancy of the inhibitor was only ~ 0.5 , although all atoms corresponding to the inhibitor were covered by electron density. We have established by 1-D and 2-D NMR, as well as by electrospray mass spectroscopy, that iodotyrostatin was the dominant component of the inhibitor used for preparing PSCP complexes, although minor components were present in the inhibitor sample (data not shown). The nature of the initial inhibitor was also confirmed by replacing it (see below) with specifically synthesized pseudo-tyrostatin that was characterized by NMR and mass spectroscopy as being very pure. With the exception of the replacement of an iodine in iodophenylalanine in P2 by a hydroxyl of tyrosine and full occupancy of the inhibitor, the electron density map of pseudo-iodotyrostatin (see Figure 2a in ref 2) is almost indistinguishable from that of pseudo-tyrostatin (Figure 3E), confirming our previously published identification of this substituent (2). In addition, when a 1:1 mixture of iodotyrostatin and pseudo-iodotyrostatin was used to replace the original inhibitor (see below), only the latter could be observed in the electron density map (not shown). When an analogous experiment was performed using tyrostatin/

pseudo-tyrostatin mixture, the electron density revealed only the former inhibitor (not shown). These effects will be further discussed below, in conjunction with the discussion of the binding constants of various inhibitors.

Interactions of the Inhibitors in the Active Site of PSCP. Although all crystals used in the experiments described here were grown from a complex with a single inhibitor, we were able to replace the original inhibitor with a number of other ones. PSCP is quite unusual in that its crystals are very stable and allow extensive modification of the mother liquor, including changes of pH by as many as 5 units, thus facilitating complete exchange of inhibitors. Indeed, the complexes obtained in the manner described under Materials and Methods had much higher occupancy of the inhibitor than the 50% reported for the original structure of PSCP. The quality of the resulting electron density maps is uniformly excellent (Figure 3), and all atoms can be unambiguously placed, with the exception of the N-terminus of chymostatin that appears to be disordered.

The linkage between the C-terminus of the inhibitors used in these studies and the OG oxygen of Ser287 is through a covalent bond to form a (reversible) hemiacetal, with the *S* stereochemistry of the carbon atom bound to the serine. An increase in pH leads to loss of the hydrogen from the $-OH$ group of the hemiacetal and expulsion of the Ser-O $-$ to reform the original aldehyde. Analogous linkages have been previously described for the complexes of chymostatin and two other serine proteinases, *Streptomyces griseus* proteinase A (13) and wheat serine carboxypeptidase II (14). The stereochemistry of the active site of PSCP is opposite to that of carboxypeptidase, in excellent agreement with the interpretation provided by Bullock et al., who noted that the arrangement of the active site residues in carboxypeptidase corresponds to a mirror image of the arrangement in subtilisin (14). Despite the similarity of the linkage, these complexes differ from the recently described peptide that was covalently bound to the active site serine of elastase (26). In that case, the carbon is planar, indicating the presence of a carbonyl rather than a hydroxyl moiety in the linkage.

The availability of the structures of a number of inhibitors allows us to delineate subsites S1–S4 of the substrate-binding site (27). In all structures compared here, the P1 residue of the inhibitor is either a tyrosine or a phenylalanine. The orientation of its side chain is virtually the same in all

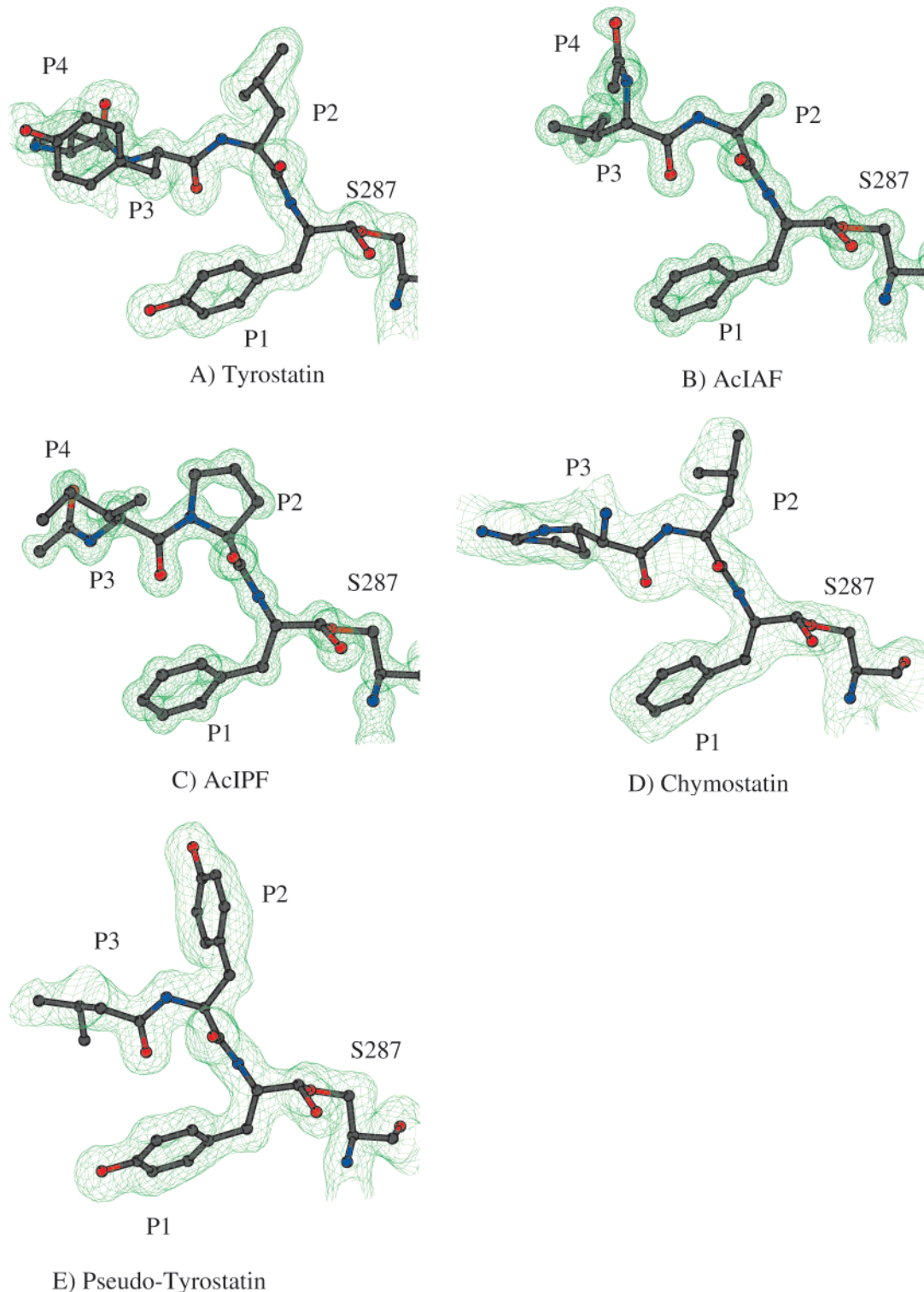


FIGURE 3: Electron density maps ($2F_o - F_c$, contoured at 1.0σ level) for the inhibitors complexed to PSCP. (A) Complex with tyrostatin; (B) complex with AcIAF; (C) complex with AcIPF; (D) complex with chymostatin; (E) complex with pseudo-tyrostatin.

complexes (Figure 4), being wedged into a pocket created by the side chain of Arg179, the main chain of residues 133–136, and the main and side chains of residues 167–170. In the inhibitors containing Tyr, its OH atom makes excellent hydrogen bonds with OE2 of Glu175 and with OG of Ser190. The structures with the P1 Phe side chain do not contain any extra water molecule(s) to compensate for the absence of OH in the side chain, since the pocket is too small to accommodate a noncovalent oxygen. It thus appears that a

tyrosine is a natural and the best substituent of the S1 subsite of PSCP.

A number of different side chains are present in the P2 position of the inhibitors, but they are all structurally superimposable (Figure 4). These residues include an iodoPhe in pseudo-iodotyrostatin (and Tyr in pseudo-tyrostatin), Leu in tyrostatin and in chymostatin, Pro in AcIPF, and Ala in AcIAF. The active site volume occupied by these residues is rather open and is bounded on one side by the

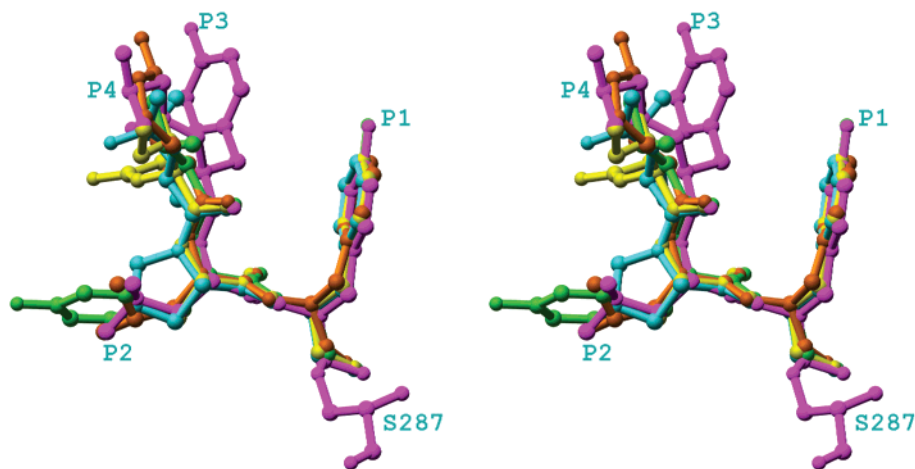


FIGURE 4: Superposition of the coordinates of the inhibitors of PSCP bound to Ser287 of the enzyme. Tyrostatin and Ser287 are shown in magenta, AcIAF in yellow, AcIPF in light blue, chymostatin in orange, and pseudo-tyrostatin in green. Only the position of Ser287 with bound tyrostatin is shown, but the orientation of its side chain is virtually identical in the other complexes.

side chains of Ile35, Asp74, Gln76, Trp81, and Glu80, while it is exposed to the solvent on the other side. The iodine of an iodoPhe and the hydroxyl of a Tyr interact with the carboxylate of Asp74. Since the P2 side chain of AcIAF consists of only a single methyl group, the rest of the S2 pocket is filled by a glycerol molecule that appears to have the right combination of hydrophobic and hydrophilic moieties to provide optimum interactions. It is not clear what other molecule(s) would substitute for glycerol that was used here only as a cryo-preservation agent, but was yet found to bind specifically.

The main chain of all the inhibitors discussed here accepts a single hydrogen bond through the P3 carbonyl oxygen from the main chain amide of Gly135 of PSCP, while a second bond is made through S3 N and 135 O in the complexes of tyrostatin and AcIPF. The space surrounding the P3 Tyr and Ile of the two latter inhibitors most likely defines the S3 area on the enzyme. That area, however, can hardly be called a pocket, since it is almost completely open. The only part of the enzyme that is in contact with the inhibitor is Arg179, but its interactions with the two types of side chains are different. The orientation of the side chain of Arg179 is almost identical in all of the complexes with the exception of tyrostatin; although it comes into contact with the Ile of AcIPF, it is not pushed from its usual location. However, the larger bulk of P3 Tyr in tyrostatin forces Arg179 to reorient. This does not seem to involve any significant input of energy, however, since that residue appears to be quite flexible, as judged by its comparatively high temperature factors (the guanidinium group had to be modeled with zero occupancy, since it was not visible in the electron density map).

The nominal positions of the P3 and P4 residues are reversed between the complexes of AcIPF and AcIAF, with the visible P3 side chain of chymostatin following the orientation of the latter. These side chains make very weak hydrophobic interactions with the side chains of Ile35, Leu114, Leu134, and Trp136 (closest interatomic distances ~ 4 Å), but, again, it is not really possible to describe an actual S4 pocket. It is clear that a variety of different side chains could be easily accommodated in this area, and thus we do not expect that this part of the inhibitor should

contribute much to its specificity (or that a corresponding residue in the substrate would contribute in a significant way to the specificity of the enzyme). In a series of octapeptide substrates substituted in P4, PSCP showed the following preferences: Pro, Leu, Ala > Ser > Asp, Arg (28).

Protonation State of the Carboxylates in PSCP. Several carboxylates in PSCP lie at close distance to each other, so that the distance between a pair of oxygens from neighboring Asp or Glu residues is less than 3.1 Å. This suggests that they are connected by a hydrogen bond and at least one carboxylate from each pair must be protonated rather than negatively charged. Several models of PSCP have been comprehensively refined at atomic resolution, in particular the native structure [PDB code 1GA6, model D (2)] at 1.0 Å, as well as models F and G from this report, both refined at 1.1 Å. At such resolution, many hydrogen atoms can be seen as peaks in the difference Fourier synthesis, mostly those connected to well-defined C α and C β atoms or peptide N atoms. Unfortunately, hydrogen atoms within hydrogen bonds are more labile and in principle can adopt one of the two positions between two electronegative parent atoms. For that reason, carboxylate hydrogens are rarely seen in the difference Fourier map.

However, there is another possibility of determining if a carboxylate group is negatively charged or not. The deprotonated carboxylate should be quite symmetric, since both its oxygen atoms are equivalent due to the resonance effect and are equidistant from carbon at 1.23 Å. Protonation takes place at one oxygen only, and breaks the symmetry of the carboxyl group, so that one oxygen atom has a double bond to carbon at 1.20 Å, and another, carrying a hydrogen, a single bond at 1.34 Å. The difference of 0.14 Å exceeds the accuracy of interatomic bonds, as estimated from the inversion of the least-squares matrix at atomic resolution. The comparison of the C–O bond lengths within carboxylate groups may indicate if they are charged or not. Such indications will not be strongly statistically validated, but nevertheless may be suggestive.

Table 2 contains the list of bond lengths in all side chain carboxylate groups in the 1GA6 model, refined at 1.0 Å, as well as corresponding distances in other high-resolution structures. Several carboxylates show marked difference

Table 2: Bond Lengths within the Carboxylate Groups^a

	native 1.0 Å		pseu-tyr 1.4 Å		AcIAF		AcIPF	
	1GA6		1GA4		1KDV		1KDY	
	C-O1	C-O2	C-O1	C-O2	C-O1	C-O2	C-O1	C-O2
Glu12	1.234	1.267?	<i>b</i>	<i>b</i>	1.242	1.288	1.237	1.289
Asp18	1.236	1.267+	1.260	1.236	1.245	1.283	1.252	1.271
Asp44	1.252	1.262-	1.261	1.247	1.262	1.266	1.255	1.283
Asp70	1.239	1.259?	1.248	1.238	1.238	1.253	1.257	1.248
Asp73	1.244	1.249-	1.256	1.251	1.265	1.242	1.268	1.264
Asp74	1.209	1.259?	1.240	1.220	1.254	1.201	1.265	1.186
Glu80	1.261	1.231+	1.284	1.283	<i>b</i>	<i>b</i>	1.275	1.265
Asp82	<i>b</i>	<i>b</i>	1.254	1.232	1.258	1.219	1.246	1.239
Asp84	1.234	1.299+	1.239	1.260	1.240	1.296	1.240	1.298
Asp105	1.256	1.237?	1.259	1.258	1.250	1.268	1.278	1.279
Asp124	1.266	1.224?	1.260	1.244	1.257	1.239	1.273	1.250
Glu138	1.257	1.246-	1.253	1.269	1.250	1.248	1.254	1.254
Asp140	1.247	1.266?	1.240	1.266	1.227	1.260	1.223	1.272
Asp144	1.244	1.251-	1.250	1.263	1.228	1.275	1.218	1.266
Glu150	1.226	1.316+	1.237	1.289	1.250	1.297	1.244	1.288
Asp151	1.256	1.240-	1.255	1.244	1.260	1.223	1.287	1.233
Asp170	1.267	1.233+	1.266	1.262	1.265	1.249	1.283	1.234
Glu171	1.262	1.287?	1.320	1.318	1.278	1.252	1.279	1.260
Glu175	1.286	1.237+	1.250	1.221	1.266	1.264	1.249	1.268
Asp183	1.260	1.249-	1.263	1.250	1.247	1.275	1.235	1.272
Glu217	1.271	1.248?	1.260	1.273	1.252	1.265	1.246	1.272
Glu222	1.275	1.255?	1.253	1.274	1.241	1.269	1.250	1.284
Asp225	1.265	1.253-	1.247	1.236	1.268	1.245	1.251	1.242
Glu241	1.308	1.232+	1.252	1.270	1.227	1.243	1.243	1.248
Asp261	1.262	1.238?	1.275	1.247	1.250	1.261	1.251	1.264
Asp265	1.214	1.317+	1.217	1.269	1.238	1.300	1.218	1.300
Asp328	1.253	1.260-	1.256	1.241	1.225	1.241	1.224	1.230
Asp348	1.247	1.267-	1.239	1.260	1.228	1.241	1.222	1.222
Asp357	1.255	1.235-	1.248	1.237	1.238	1.244	1.237	1.251

^a The names of the carboxylate atoms are taken from the structure of AcIAF (PDB code 1KDV). Note that the nomenclature used in the previously deposited models of PSCP (PDB codes 1GA1, 1GA4, and 1GA6) is not consistent with the IUPAC rules for naming of the carboxylates, but that it has been corrected in the coordinate sets. The errors of atomic positions in the 1.0 Å native structure are about 0.02 Å. Abbreviations: +, suggesting -COO protonated; -, suggesting -COO ionized; ?, no decisive indication. ^b Disordered.

between both C-O bonds, considerably exceeding the estimated bond length error. The protonated carboxylates are those that are involved in hydrogen bonds between neighboring Asp and Glu residues, and it is possible to describe several networks of hydrogen bonds (Figure 5). The two aspartate side chain carboxylates coordinating the calcium ion (Asp328 and Asp348) must be charged, and indeed they have similar C-O bond lengths, providing indirect validation of this analysis. While this analysis is at this time relevant primarily to the native structure, we hope that a similar approach to inhibitor complexes may ultimately help in delineating more details of the catalytic mechanism of PSCP.

Catalytic Site of PSCP. As established by us previously, the primary residues that constitute the catalytic site of PSCP are Ser287, Glu80, and Asp84. In all covalent complexes described here and in the previous report (2), Ser287 is covalently bound to the aldehyde group at the C-terminal end of each inhibitor. The OG atom of the side chain occupies a single position in all of the complexes studied here (models E-I, Table 1), while two orientations were present in the partially occupied complex with pseudoiodotyrosatin (model B in the previous study). All three common rotamers of the side chain of this residue were observed in the atomic-resolution structure of uninhibited PSCP (model D from the previous study). When in its most conserved orientation, the OG atom of Ser287 is hydrogen-

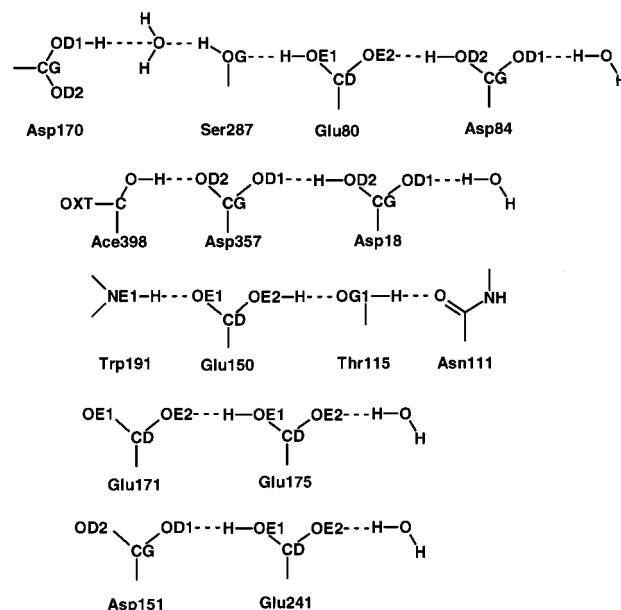


FIGURE 5: Probable hydrogen-bonded networks involving side chain carboxylate residues in the 1.0 Å resolution structure of uninhibited PSCP (PDB accession code 1GA6). This figure was based on data shown in Table 2.

bonded to OE1 of Glu80 (see above), initiating a chain of hydrogen-bonded interactions necessary to establish catalytic activity. The OE2 atom of Glu80, in turn, is hydrogen-bonded to OD2 of Asp84.

Whereas the positions of the CA and CB atoms of Ser287, as well as the complete side chain of Asp84, are virtually identical in all structures of PSCP, whether inhibited or not, the side chain of Glu80 assumes double conformations in the complexes with AcIAF and AcIPF. One of these conformations is the common one described above, while the other breaks the chain of hydrogen-bonded interactions between active site residues. It is likely that these multiple conformations result from the change in the protonation state of Glu80 in these complexes, but it is not clear at this time why similar phenomena are not observed with tyrostatin or chymostatin.

At least one other residue can be unambiguously defined as being crucial for the catalytic activity of PSCP. This residue is Asp170, structurally equivalent to Asn155 in subtilisin. The orientation of the side chain of Asp170 is virtually identical in all the inhibitor complexes of PSCP studied to date, as well as in the uninhibited enzyme. The side chain of Asn155 in subtilisin creates part of the oxyanion hole stabilizing the tetrahedral intermediate of the reaction. The orientation of the side chain relative to the covalently bound inhibitor is the same in both subtilisin and PSCP.

K_i Values and Mode of Inhibition. The first known inhibitor of PSCP was tyrostatin, isolated from culture filtrates of *Kitasatosporia* (25). Tyrostatin had the ability to inhibit the activity of PSCP [$K_i = 2.6$ nM (29)] as well as XSCP [$K_i = 2.1$ nM (28)]. The structure of tyrostatin was determined to be isovaleryl-Tyr-Leu-tyrosinal (Figure 1A). In Table 3 we present K_i values determined in the current study under uniform conditions for tyrostatin and for the other aldehyde inhibitors discussed above. These values were obtained by treating the compounds as reversible competitive inhibitors. Attempts to measure the inhibition as a rate

Table 3: Determination of the Inhibition Constants for a Series of Inhibitors of PSCP^a

inhibitor	K_i (nM)
tyrostatin	6 ± 0.5
psuedo-tyrostatin	56 ± 7
iodotyrostatin	32 ± 5
pseudo-iodotyrostatin	14 ± 1.5
chymostatin	45 ± 6
AcIPF	415 ± 93
AcIAF	600 ± 55

^a Chemical formulas for these inhibitors are shown in Figure 1.

process by observing an increase in the level of inhibition with time of incubation were unsuccessful. Apparently, equilibrium is reached within the 10 min incubation time that is necessary to bring all reactants in the enzymatic assay to 37 °C. The assumption of reversibility in the reaction between the OG of Ser287 and the carbonyl carbon to produce a hemiacetal product is confirmed by the observation that an increase in pH will permit dissociation of the inhibitor from the active site.

Comparison of tyrostatin and pseudo-tyrostatin shows that the latter compound binds significantly weaker; this could be due either to a less optimal fit of Tyr compared to Leu in S2 or to the less optimal fit of the isovaleryl group compared to Tyr in S3. It is possible that the interaction of Arg179 with the aromatic ring of tyrostatin in S3 provides some stabilization. Strikingly, however, the situation is entirely different in comparing iodotyrostatin with pseudo-iodotyrostatin, with the shorter inhibitor yielding a lower value of K_i . In comparing tyrostatin and iodotyrostatin, it can be seen that Tyr is a better P3 substituent than iodoPhe, indicating that the slightly larger iodoPhe may destabilize the complex. Comparing pseudo-tyrostatin and pseudo-iodotyrostatin shows that iodoPhe is better in P2 than Tyr. This indicates that the lower K_i value for pseudo-iodotyrostatin is due to a combination of both weak binding of iodoPhe in P3 and better binding of iodoPhe in P2.

AcIAF and AcIPF were synthesized as potential inhibitors of KSCP, as it was observed that tyrostatin did not inhibit KSCP and a related enzyme, J-4. In addition, it was reported that synthetic peptide substrates containing Ala or Pro in P2 are optimal for KSCP (30) while substrates with Leu in P2 are better for PSCP (31). This distinction is perfectly mirrored in the K_i values reported in Table 3 in that AcIAF and AcIPF are considerably weaker inhibitors of PSCP than inhibitors with Leu, Tyr, iodoPhe, or Ile in the P2 position. Surprisingly, although chymostatin is a nonspecific inhibitor of a variety of serine proteinases, its binding to PSCP is quite strong.

In the previously described structures of inhibitor complexes of PSCP (2), fragments of the inhibitor were also seen in one of the crystals in a very different orientation than the one described above. There was no indication of any covalent bond between the inhibitor and Ser287, and the visible portion of the inhibitor, consisting of the iodoPhe residues and the main chain atoms of the adjacent residues (modeled as glycines), occupied parts of the P1'-P3' pockets. The side chain of the P2' residue was making excellent parallel stacking interactions with the indole ring of Trp231, and perpendicular interactions with Trp220. This noncovalent inhibitor provided at least a glimpse of the prime binding

site, not directly targeted by the series of inhibitors used in these studies.

CONCLUSIONS

This report resolves our somewhat perplexing observation that pseudo-iodotyrostatin, a minor (<5%) component of a synthetic preparation of iodotyrostatin, was bound into the active site of PSCP, instead of the major component, iodotyrostatin. Pseudo-tyrostatin and pseudo-iodotyrostatin place larger groups into the S2 active site pocket, and the latter inhibitor also avoids an unfavorable interaction in S3. Our observation of hemiacetals with Ser287 for all inhibitor complexes reinforces our previous conclusions (2) that this residue must be the catalytic group of enzymes in the S53 family (32). Additional work underway with KSCP confirms these observations (W. Bode, personal communication; and K. Oda, unpublished results). Obtaining structural information at high-to-atomic resolution has allowed an analysis of hydrogen bonding patterns and, hence, contributed to mechanistic analysis. By analogy, we anticipate that the medically important human enzyme, CLN2, will follow a similar mechanism involving a Ser-Glu-Asp catalytic triad with oxyanion stabilization/protonation by the residue equivalent to the absolutely conserved Asp170, and that modeling of its structure and predicting the specificity should now be possible.

ACKNOWLEDGMENT

We thank Jerry Alexandratos for help in preparation of the figures.

REFERENCES

- Dauter, Z., Li, M., and Wlodawer, A. (2001) *Acta Crystallogr. D57*, 239–249.
- Wlodawer, A., Li, M., Dauter, Z., Gustchina, A., Uchida, K., Oyama, H., Dunn, B. M., and Oda, K. (2001) *Nat. Struct. Biol.* 8, 442–446.
- Oda, K., Sugitani, M., Fukuhara, K., and Murao, S. (1987) *Biochim. Biophys. Acta* 923, 463–469.
- Oda, K., Takahashi, T., Tokuda, Y., Shibano, Y., and Takahashi, S. (1994) *J. Biol. Chem.* 269, 26518–26524.
- Ito, M., Narutaki, S., Uchida, K., and Oda, K. (1999) *J. Biochem. (Tokyo)* 125, 210–216.
- Oyama, H., Abe, S., Ushiyama, S., Takahashi, S., and Oda, K. (1999) *J. Biol. Chem.* 274, 27815–27822.
- Murao, S., Ohkuni, K., Nagao, M., Hirayama, K., Fukuhara, K., Oda, K., Oyama, H., and Shin, T. (1993) *J. Biol. Chem.* 268, 349–355.
- Shibata, M., Dunn, B. M., and Oda, K. (1998) *J. Biochem. (Tokyo)* 124, 642–647.
- Rawlings, N. D., and Barrett, A. J. (1999) *Biochim. Biophys. Acta* 1429, 496–500.
- Lin, L., Sohar, I., Lackland, H., and Lobel, P. (2001) *J. Biol. Chem.* 276, 2249–2255.
- Sleat, D. E., Donnelly, R. J., Lackland, H., Liu, C. G., Sohar, I., Pullarkat, R. K., and Lobel, P. (1997) *Science* 277, 1802–1805.
- Kwon, H. K., Kim, H., and Ahn, T. I. (1999) *Korean J. Biol. Sci.* 3, 221–228.
- Delbaere, L. T., and Brayer, G. D. (1985) *J. Mol. Biol.* 183, 89–103.
- Bullock, T. L., Breddam, K., and Remington, S. J. (1996) *J. Mol. Biol.* 255, 714–725.
- Parikh, J. R., and Doering, W. E. (1967) *J. Am. Chem. Soc.* 89, 5505–5507.
- Hamada, Y., and Shioiri, T. (1982) *Chem. Pharm. Bull. (Tokyo)* 30, 1921–1924.

17. Otwinowski, Z., and Minor, W. (1997) *Methods Enzymol.* 276, 307–326.
18. Sheldrick, G. M., and Schneider, T. R. (1997) *Methods Enzymol.* 277, 319–343.
19. Jones, T. A., and Kieldgaard, M. (1997) *Methods Enzymol.* 277, 173–208.
20. Engh, R., and Huber, R. (1991) *Acta Crystallogr. A* 47, 392–400.
21. Robertus, J. D., Kraut, J., Alden, R. A., and Birktoft, J. J. (1972) *Biochemistry* 11, 4293–4303.
22. Matthews, D. A., Alden, R. A., Birktoft, J. J., Freer, S. T., and Kraut, J. (1975) *J. Biol. Chem.* 250, 7120–7126.
23. Wright, C. S., Alden, R. A., and Kraut, J. (1972) *J. Mol. Biol.* 66, 283–289.
24. Kuhn, P., Knapp, M., Soltis, S. M., Ganshaw, G., Thoene, M., and Bott, R. (1998) *Biochemistry* 37, 13446–13452.
25. Oda, K., Fukuda, Y., Murao, S., Uchida, K., and Kainosho, M. (1989) *Agric. Biol. Chem.* 53, 405–415.
26. Wilmouth, R. C., Edman, K., Neutze, R., Wright, P. A., Clifton, I. J., Schneider, T. R., Schofield, C. J., and Hajdu, J. (2001) *Nat. Struct. Biol.* 8, 689–694.
27. Schechter, I., and Berger, A. (1967) *Biochem. Biophys. Res. Commun.* 27, 157–162.
28. Ito, M., Dunn, B. M., and Oda, K. (1996) *J. Biochem. (Tokyo)* 120, 845–850.
29. Oda, K., Nakatani, H., and Dunn, B. M. (1992) *Biochim. Biophys. Acta* 1120, 208–214.
30. Oda, K., Ogasawara, S., Oyama, H., and Dunn, B. M. (2000) *J. Biochem. (Tokyo)* 128, 499–507.
31. Narutaki, S., Dunn, B. M., and Oda, K. (1999) *J. Biochem. (Tokyo)* 125, 75–81.
32. Rawlings, N. D., and Barrett, A. J. (2000) *Nucleic Acids Res.* 28, 323–325.

BI011817N